



HAL
open science

Study of the spontaneous nano-emulsification process with different octadecyl succinic anhydride derivatives

Xinyue Wang, Mayeul Collot, Thierry F Vandamme, Nicolas Anton

► **To cite this version:**

Xinyue Wang, Mayeul Collot, Thierry F Vandamme, Nicolas Anton. Study of the spontaneous nano-emulsification process with different octadecyl succinic anhydride derivatives. *Colloids and Surfaces A: Physicochemical and Engineering Aspects*, 2022, 645, 10.1016/j.colsurfa.2022.128858 . hal-03842754

HAL Id: hal-03842754

<https://hal.science/hal-03842754v1>

Submitted on 8 Nov 2022

HAL is a multi-disciplinary open access archive for the deposit and dissemination of scientific research documents, whether they are published or not. The documents may come from teaching and research institutions in France or abroad, or from public or private research centers.

L'archive ouverte pluridisciplinaire **HAL**, est destinée au dépôt et à la diffusion de documents scientifiques de niveau recherche, publiés ou non, émanant des établissements d'enseignement et de recherche français ou étrangers, des laboratoires publics ou privés.

Study of the spontaneous nano-emulsification process with different octadecyl succinic anhydride derivatives

Xinyue Wang,^a Mayeul Collot,^{b,*} Thierry F. Vandamme,^{a,c} Nicolas Anton^{a,c,*}

^a *Université de Strasbourg, CNRS, CAMB UMR 7199, F-67000 Strasbourg, France*

^b *Université de Strasbourg, CNRS, LBP UMR 7021, F-67000 Strasbourg, France*

^c *INSERM (French National Institute of Health and Medical Research), UMR 1260, Regenerative Nanomedicine (RNM), FMTS, Université de Strasbourg, F-67000 Strasbourg, France*

* To whom correspondence should be addressed: Nicolas Anton (nanton@unistra.fr) and Mayeul Collot (mayeul.collot@unistra.fr)

Abstract

Three new amphiphilic molecules were synthesized on a basis of a common monomer, octadecyl succinic anhydride (OSA), on which were grafted different PEGylated hydrophilic polar head. The objective of this study is to investigate a potential relationship between the chemical structure of the surfactant, and the efficiency to generate nano-emulsions through the spontaneous nano-emulsification method. Beyond the innovative synthesis and comparison of these amphiphiles, a comprehensive comparison is suggested, comparing size distribution and polydispersity for the different composition parameters, as well making a bridge with critical micelle concentration and hydrophile lipophile balance (HLB). Using OSA monomeric entity as common hydrophobic moiety, the variations in the surfactant molecules were done on the hydrophilic moiety, through the addition of one or two Jeffamine chains in different configurations, so-called C_{18}^{\ominus} -PEG, C_{18} -PEG and C_{18} -PEG₂. The results disclosed that C_{18}^{\ominus} -PEG allows producing smallest size distribution and lowest PDI values. Moreover, C_{18}^{\ominus} -PEG presents the highest critical micellar concentration, linked to a higher hydrophilicity of the molecule. This impacts the balance between surfactant affinity for oil and aqueous phases, a point probably related to the spontaneous emulsification efficiency. A last part of the study regarded the optimization of the emulsification efficiency, through a systematic study in ternary composition map, to disclosed that the best conditions are included in the lower surfactant concentrations, for water and oil contents higher and lower than 50%, respectively. The main idea behind this study was to bring further insights into the unclear relationship between the chemical structure of nonionic surfactants, and the efficiency of the emulsification by spontaneous low-energy method.

37 **1 Introduction**

38 Nano-emulsions (NEs) consist of a colloidal dispersion of two immiscible liquids stabilized by
39 amphiphilic molecules, sizing from around 30 nm to 300 nm [1]. Owing to the high surface
40 area, good physical stability, non-irritant and non-toxicity, and tunable properties, NEs are
41 becoming promising carriers for bioactive compounds and have been extensively
42 investigated in many fields such as drug delivery, diagnostic, cosmetic, pesticide and food
43 industry [2–6].

44 Comparing with conventional high-energy methods, like high pressure homogenization,
45 ultrasound emulsification, membrane emulsification etc., such low-energy emulsification
46 requires a very limited addition of external energy, but takes advantages of the physico-
47 chemical properties of the compounds to fractionate the oil phase at nano-metric scale. One
48 advantage of this concept lies in the fact that fragile pharmaceutical ingredients are
49 preserved from a potential degradation due to high local energy amount supplied with
50 mechanical homogenization [7]. However, these methods are still not largely used in industry
51 [8], since (i) not all surfactants allows an efficient spontaneous emulsification, (ii) the
52 physicochemical properties of the NEs dispersion cannot always be finely controlled, in term
53 of size and dispersity, and (iii) they involve a significant amount of surfactants, not always
54 compatible with all applications and specifications. Further investigations on the
55 spontaneous emulsification process are then necessary to increase the understanding of the
56 role of surfactant in the process, in order to optimize the applicability of such a low-energy
57 process.

58 Spontaneous emulsification, or self-emulsification, is performed by gently mixing two liquid
59 phases containing specific surfactants (and/or co-solvents) without any extra energy supply.
60 Spontaneous emulsification was firstly discovered by Johannes Gad in 1879 and has been
61 extensively studied in the last few decades [1,9,10]. Mechanisms behind spontaneous
62 emulsification has been described according to several hypotheses [10,11], originated from
63 interfacial turbulence phenomena, generation of ultralow interfacial tensions, or explained
64 through the solubility changes and sudden migration of the nonionic surfactant in the
65 different phases in presence.

66 General experimental observations of spontaneous emulsification process give that the main
67 parameters influencing the nano-emulsion size and properties are the compositions and
68 chemical nature of surfactants and oils, temperatures or order of mixing of the different
69 compounds [1,12]. Nevertheless, an universal mechanism has been proposed, based on the
70 respective affinities between surfactants, oils and water phases [1]. The idea proposed a
71 sudden change of the thermodynamic conditions inducing a rapid change of the solubility for
72 surfactant for oil or water, and inducing a turbulence in the system leading to break-up the

73 oil phase into nano-droplets. This clearly places the surfactant solubility and its temperature
74 sensitivity, as critical for the efficiency of the spontaneous emulsification.

75 The spontaneous process is related to the sensitivity of the nonionic surfactant (precisely of
76 the poly(ethylene glycol) polar head of the molecule) with the temperature. The most
77 reported examples use commercial surfactant like, *e.g.*, polysorbate (Tween®), sorbitan
78 esters (Span®), polyoxyl 35 castor oil (Kolliphor® EL/ELP) and poloxamer (Pluronic® F68).
79 Upon temperature increasing, these surfactants lose their solubility in water to the benefit of
80 the lipophilic part. As a consequence of the gradual decrease of the number of hydrogen
81 bounding between PEG chain and water molecules, the PEG solubility is reduced. Then,
82 nano-emulsion is generated as a result of a temperature decrease and/or water dilution,
83 resulting from an increase of the solubility of these nonionic surfactants in water [13].

84 On the other hand, in spite of the number of studies to explain these spontaneous
85 emulsification mechanisms, in spite of the understanding of the impact of the formulation
86 parameters on the size and polydispersity of the nano-emulsion, a part of this concept is still
87 unclear including the relationship between the process efficiency and the chemical nature of
88 both the oil and the surfactants.

89 The spontaneous emulsification is generally considered to be driven by the affinities
90 between oil and surfactants, impacted by a change of their chemical nature of the former
91 and/or the latter. For instance as regard the impact of the nature of oil, spontaneous
92 emulsification processes reported with castor oil and modified castor oil (tri-iodinated castor
93 oil, in Fig. 2 (b₁) of Ref. [14]), not only shows a significant shift of the nano-emulsion droplet's
94 size of around 100 nm, but also significantly reduces the domain of emulsification process
95 comparing native and modified oil. This observation is recurrent with numerous types of oil
96 phases, an interesting example is the one of *α-tocopherol*, for which the spontaneous
97 emulsification process is not giving nano-scaled droplets —but rather large micrometric
98 droplets— and for which acetate form [15,16] or tri-iodinated form [17,18] is extremely
99 efficient and gives rise to very small (< 50 nm) and very narrow size distribution (PDI < 0.1).

100 Some reports have emphasized that in the case of spontaneous emulsification where the
101 free energy cost for creating the interfacial area has to be compensated by a large entropic
102 term, thus a flexible surfactant allowing curvature fluctuations is required [19]. Small
103 monomeric surfactants adsorb on the interface of newly form droplets very quickly and
104 result in the production of small droplets, while comparatively polymer generally giving
105 larger droplet size range, *i.e.* inappropriate for the formation of nano-emulsions [20]. Besides
106 the experimental comparison of the results given by nonionic surfactants, comparing each
107 other upon the nano-emulsification process, *predicting* the compatibility of these molecules
108 with spontaneous emulsification process remains, to date, unclear in literature.

109 In the present study we have synthesized different nonionic surfactants with slight
110 modifications in their chemical structure, and they were compared upon the spontaneous
111 emulsification process. Beside the formulation of NEs, the goal is to understand the impact
112 of the change in the surfactant structure in the efficiency of the process, as well as size and
113 dispersity of the droplet population. The main objective of our investigation here lies in
114 highlighting potential relationship between chemical structure of surfactant and efficiency of
115 emulsification. We have chosen to synthesize octadecyl succinic anhydride derivatives with
116 different functions including grafting of nonionic polymers. It is noteworthy that these new
117 surfactants are not exactly the same as the commercial ones –however very close in the
118 chemical structure principle– but our idea was to get a series of molecules very close each
119 other only differing in one chemical function, to compare them as regards the emulsification
120 efficiency.

121

122

123 **2 Materials and methods**

124 **2.1 Materials**

125 Octadecyl succinic anhydride (OSA) and vitamin E acetate (VEA) were purchased from Tokyo
126 Chemical Industry. Polyetheramine Jeffamine[®] M-2070 (J-2000) was kindly offered by
127 Huntsman Corporation. Ethanol, ethanolamine, triethylamine (TEA), dimethylformamide
128 (DMF), dichloroform (DCM) and hexafluorophosphate azabenzotriazole tetramethyl uranium
129 (HATU) were obtained from Merck-Millipore. Phosphate buffered saline (PBS) was from
130 Eurobio (Courtaboeuf, France).

131 **2.2 Synthesis**

132 The structures of three amphiphilic molecules specially synthesized for this study, so-
133 called C_{18}^{\ominus} -PEG, C_{18} -PEG and C_{18} -PEG₂, are illustrated in Fig. 1, and the synthesis procedures
134 are described below. These surfactants arise from the reaction of the amine (NH₂)
135 terminated PEG (J-2000) on amine-reactive anhydride (OSA) first providing C_{18}^{\ominus} -PEG, which
136 thus bears a carboxylic acid function. This function was then either reacted with another J-
137 2000 (forming C_{18} -PEG₂), or capped with ethanolamine (forming C_{18} -PEG).

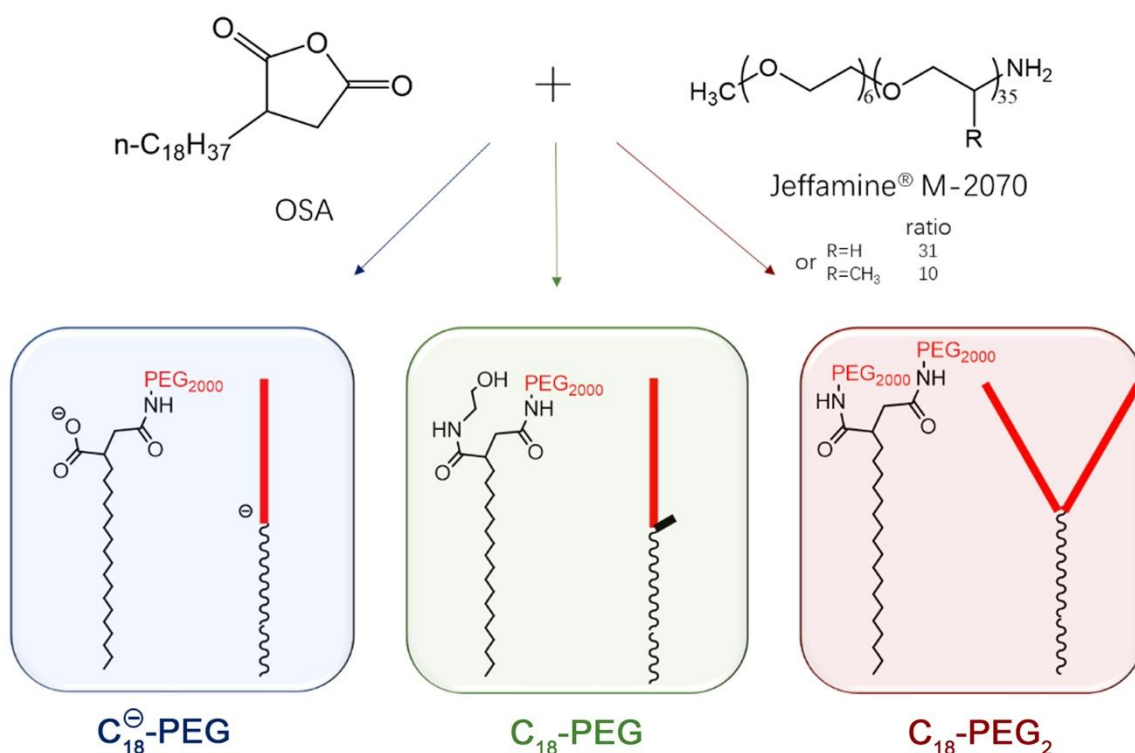
138 **C_{18}^{\ominus} -PEG:** To a solution of OSA (352 mg, 1 mmol) in DMF (20 mL) was added J-2000 (2 g, 1
139 mmol) dissolved in DMF (10 mL). After the homogeneity, 696 μ L of TEA (5 mmol, 5 eq) were
140 added to the solution following a heating up to 60°C overnight. Then, the solvent was
141 evaporated. For the purification, firstly, the crude was dissolved in DCM, and then washed

142 three times by 1 M HCl in saturated NaCl solution. The organic phase was dried over
143 anhydrous sodium sulfate, filtrated over cotton and evaporated.

144 **C₁₈-PEG₂**: To a solution of OSA (352 mg, 1 mmol) in DMF (20 mL) was added J-2000 (4 g, 2
145 mmol, 2 eq) dissolved in DMF (20 mL). After the homogeneity, 696 μ L of TEA (5 eq) and HATU
146 (570 mg, 1.5 eq) were added to the solution following a heating up to 60°C overnight. Then,
147 the solvent was evaporated. For the purification, firstly, the crude was dissolved in ethanol,
148 and then dialysis was conducted with a regenerated cellulose membrane (molecular weight
149 cutting off is 2,000 Da). Outside media (ethanol) was changed every 8 h for 3 times. The final
150 product was obtained with evaporation of ethanol.

151
152 **C₁₈-PEG**: To a solution of OSA (352 mg, 1 mmol) in DMF (20 mL) was added J-2000 (2 g, 2
153 mmol, 2 eq) dissolved in DMF (10 mL). After the homogeneity, 696 μ L of TEA (5 eq) was
154 added to the solution following a heating up to 60°C overnight. Then, 60 μ L of ethanolamine
155 (1 eq dissolved in 5 mL DMF) and HATU (570 mg, 1.5 eq) were added to the solution at the
156 same temperature overnight again. Next, the solvents were evaporated, and the purification
157 was strictly the same as described for **C₁₈-PEG₂**.

158



159
160 **Figure 1:** Synthesis and structure scheme of the three amphiphilic molecules synthesized. Red chain symbolizes
161 the PEG chains.

162

163 2.3 Structure confirmation

164 To confirm the structure of three molecules, around 40 mg of products were dissolved in
165 500 μL CDCl_3 for NMR tests. Both ^1H -NMR and ^{13}C -NMR spectra were recorded on a Bruker
166 Avance III 400 MHz spectrometer.

167

168 2.4 Critical micelle concentration (CMC) determination

169 The CMC of three amphiphilic molecules were determined by a fluorescence method using
170 Nile red (NR) as a probe [21]. NR in DMSO (200 μM) was used as a stock solution. Firstly, a
171 series of 1 mL solutions of each surfactant (with concentrations ranging from 0.001 to 10
172 mg/mL) in milliQ water were prepared, and 5 μL of NR stock solution were added into each
173 sample to reach a final NR concentration of 1 μM . Fluorescence spectra were recorded at
174 20°C at a fixed excitation of 530 nm, and the emission was monitored from 540 nm to 800
175 nm. The maximum emission wavelength (λ_{em}) was recorded and presented for the CMC
176 calculation, corresponding to the intercept between the straight baseline (before CMC) and
177 the rising straight line of the fluorescence signal (after CMC).

178

179 2.5 hydrophile lipophile balance (HLB) calculation

180 HLB values of each amphiphilic molecule were calculated according to the commonly used
181 Davies' group contribution method [22]. Details of the equation and table of parameters are
182 reported in the *Supplementary information* section, Eq. S1 and Table S1, respectively.

183 2.6 Emulsification

184 Spontaneous emulsification method was used as reported in previous papers [16,23]. In
185 brief, surfactants were dissolved in oil phase with different *surfactant to oil weight ratio*
186 (SOR) at a set temperature, then PBS, maintained at the same temperature, was added
187 according to different *(surfactant + oil) to water weight ratio* (SOWR). After vortex
188 homogenization for 1 min, following a mixing in a thermomixer at 2,000 rpm for 10 min
189 nano-emulsions were formed. In order to explore and optimize the emulsification conditions,
190 the process was performed at different compositions and environmental conditions.

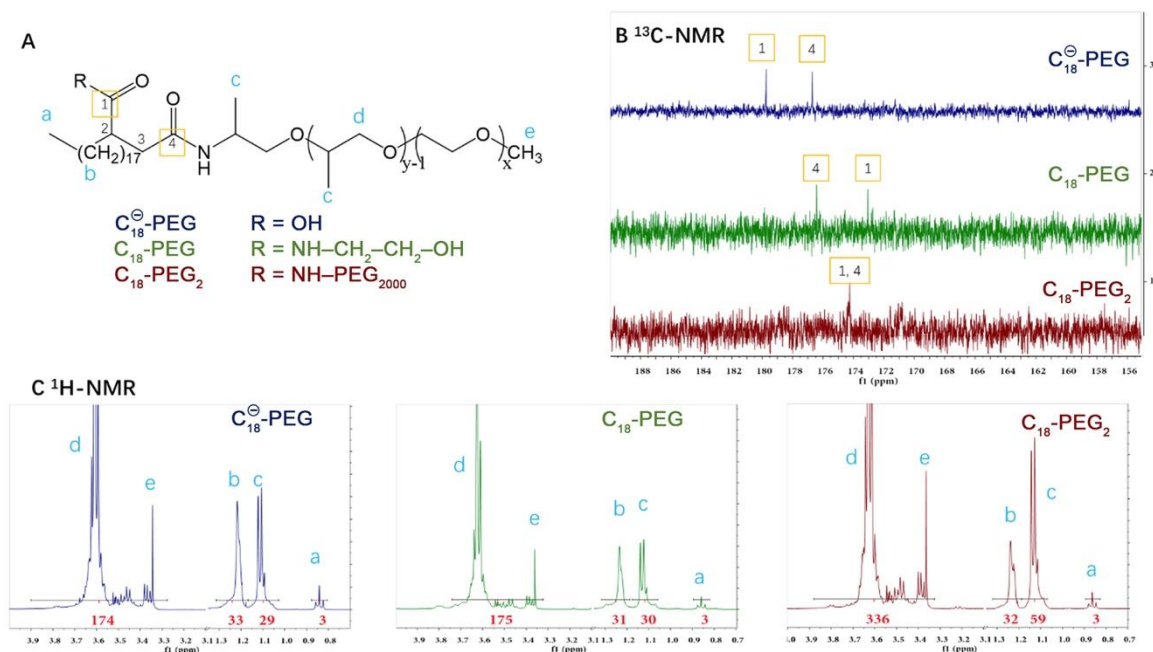
191 Size distribution, polydispersity index and ξ potential were determined by dynamic light
192 scattering (DLS) with NanoZS (Malvern, Orsay, France). Generated emulsions were diluted by
193 100 and 1,000 times in distilled water, for size and ξ potential measurements, respectively.

194

195 3 Results and discussion

196 3.1 Structure identification of new molecules

197 Due to the simple synthesis process, the reaction yield for each molecule was above 90%.
198 Structures of the three amphiphilic molecules are shown in Fig. 1. With the similar
199 hydrophobic saturated aliphatic chain (shown in black), the difference in these molecules
200 arose in their hydrophilic head (red). Three different variations (see Fig. 1) of their polar head
201 compositions came from the fact that C_{18}^{\ominus} -PEG beared a -COOH, potentially becoming
202 carboxylate when solvated at the oil/water interface and in PBS (pH 7.4), while for C_{18} -PEG,
203 the capped ethanolamine part annihilated the charge, and for the C_{18} -PEG₂ the carboxylic
204 acid was replaced by another J-2000. The structures were unambiguously identified by ¹H
205 and ¹³C NMR spectra (the identical parts shown in Fig. 2, while the complete spectra were
206 reported in the *Supplementary information* section). It followed that, as C_{18}^{\ominus} -PEG and C_{18} -
207 PEG are shown to bear two different amide moieties (carbon 1 and 4 shown in Fig. 2A), two
208 different carbonyl signals could be observed in ¹³C NMR (δ 179.83 and 176.78 ppm for C_{18}^{\ominus} -
209 PEG, 176.53 and 173.17 ppm for C_{18} -PEG). On the contrary, C_{18} -PEG₂ only showed one
210 carbonyl signal at 174.27 ppm due to the similarity of the amide moieties (Fig. 2B). In
211 addition, in Fig. 2C, integration of the number of protons (¹H NMR) of the PEG moieties
212 appeared consistent with their supposed structure: proton intergrations at ~1.1 ppm (peaks c)
213 and ~3.6 ppm (peaks d and e) appeared twice higher for C_{18} -PEG₂, which have two PEG
214 chains, compared to C_{18}^{\ominus} -PEG and C_{18} -PEG having one PEG chain.



215
216 **Figure 2:** NMR spectra of three synthesized surfactants.

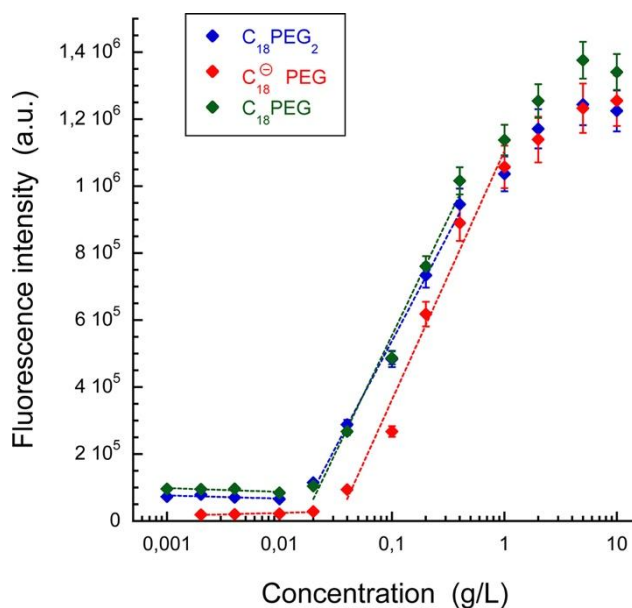
217

218 3.2 Physico-chemical characterization of the surfactants

219 Physicochemical properties of surfactants are crucial to understand their behavior and
220 potential applications, along with the fact that they play a critical role on structure-activity
221 relationship screening. Beside appearance and molecular weight, CMC and HLB were
222 determined, allowing a first comparison. Results concerning the determination of CMC are
223 reported in Fig. 3 and all data summarized in table 1 (see details regarding the fluorescent
224 spectra are reported in Fig. S1, in the *Supplementary Information* section). HLB values were
225 rather comparable between C_{18}^{\ominus} -PEG, C_{18} -PEG (12.3 and 14.3, respectively), but increased
226 up to 22.8 for C_{18} -PEG₂ respectively. All these surfactants had a HLB value significantly high,
227 enough to be considered as very hydrophilic, compatible with application as stabilizer for
228 direct emulsification. Interestingly, the HLB value of C_{18} -PEG₂ jumped to 22.8, significantly
229 higher than the two formers. As regards the CMC values, a significant gap appeared between
230 the neutral (C_{18} -PEG and C_{18} -PEG₂ around 0.02 g/L) and charged surfactants (C_{18}^{\ominus} -PEG
231 around 0.036 g/L), reflecting the higher solubility of the molecule coming from its ionic
232 nature. Indeed, the higher the water solubility, the higher the CMC, as described in literature
233 [24]. As a last remark, the comparison of the CMC and HLB values were not exactly inline
234 each other, likely explained by the fact that HLB remained calculations based on chemical
235 structure, whereas CMC determination was based on the actual experimental behavior.
236 Nevertheless, HLB values of all these surfactants indicated they are very hydrophilic
237 molecules.

238

239



240

241 **Figure 3:** Determination of the Critical Micelle Concentration of the different amphiphile molecules, using Nile
242 Red as fluorescent probe (see details in the text, *section 2.4*).

243

244 **Table 1:** Physicochemical properties of three new surfactants

Product	Appearance (R.T.)	M.W.	CMC (20°C)	HLB
C₁₈[⊖]-PEG	white-yellowish paste	~2300	0.036 mg/ml	12.3
C₁₈-PEG	white-yellowish wax	~2350	0.021 mg/ml	14.3
C₁₈⁺-PEG₂	yellow wax	~4300	0.018 mg/ml	22.8

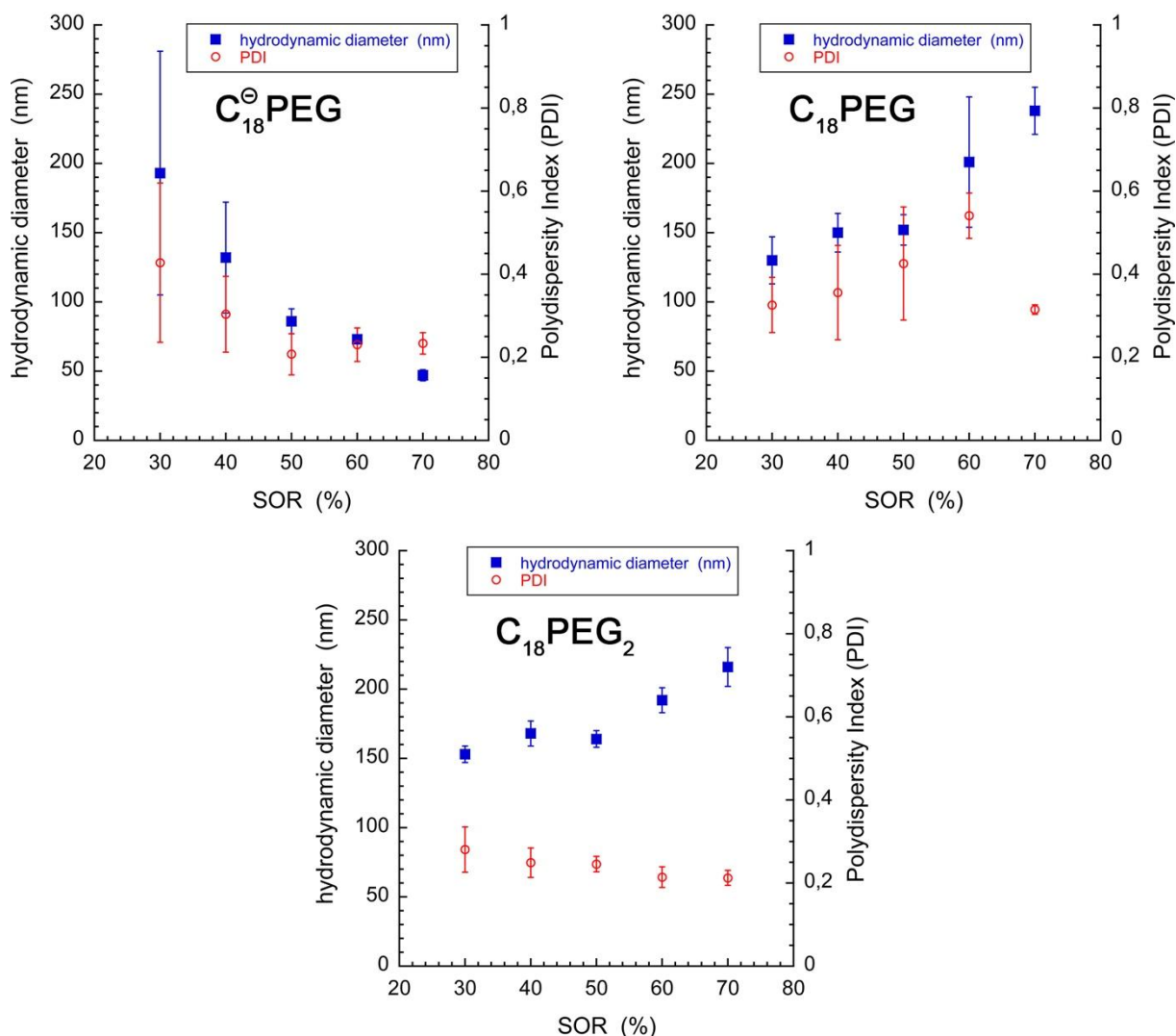
245

246 3.3 Emulsification efficiency of three surfactants

247 Although spontaneous emulsification provided a much convenient and economic method for
 248 nano-emulsification, the formulation was not as predictable as the mechanical methods. The
 249 general route to study spontaneous emulsification process was generally done [1] following-
 250 up of the size distribution of the nano-emulsions along with modifications of compositions
 251 parameters like surfactant amount (with SOR), dispersed volume fraction (with SOWR), or
 252 environment parameters like, *e.g.*, temperature. These key parameters were investigated for
 253 that purpose, with the idea to disclose the structure-properties relationship.

254

3.3.1 Effect of surfactant concentration



256

257 **Figure 4:** Size and PDI of NEs prepared using C_{18}^{\ominus} -PEG, C_{18} -PEG and C_{18} -PEG₂, in function of the values of SOR,
 258 at constant SOWR = 5% and at emulsification temperature $T = 90^{\circ}\text{C}$.

259

260 For this first series of experiments, the SOR (linked to surfactant amount) was gradually
 261 increased and the size distribution (*i.e.* average diameter and polydispersity indexes (PDI))
 262 was measured. Thus, SORs varied from 30% to 70%, at a fixed SOWR of 5% and a fixed
 263 temperature of the emulsification process of 90°C , temperature at which both the {oil +
 264 surfactant} and the water phases were maintained before mixing. Results were reported in
 265 Fig. 4. The case of C_{18}^{\ominus} -PEG (Fig. 4A) showed the most conventional behavior compared to
 266 literature [1,25], where increasing the SOR value induced a decrease in the mean droplet's
 267 size and PDI. Reproducibility was improved with SOR. It is important to note that nano-
 268 emulsions were considered monodispersed, and therefore the spontaneous process
 269 considered as efficient, when the PDI was lower than 0.25; in that case, this criterion was
 270 met for $\text{SOR} > 50\%$, when the droplet size decreased below 90 nm. This trend was generally

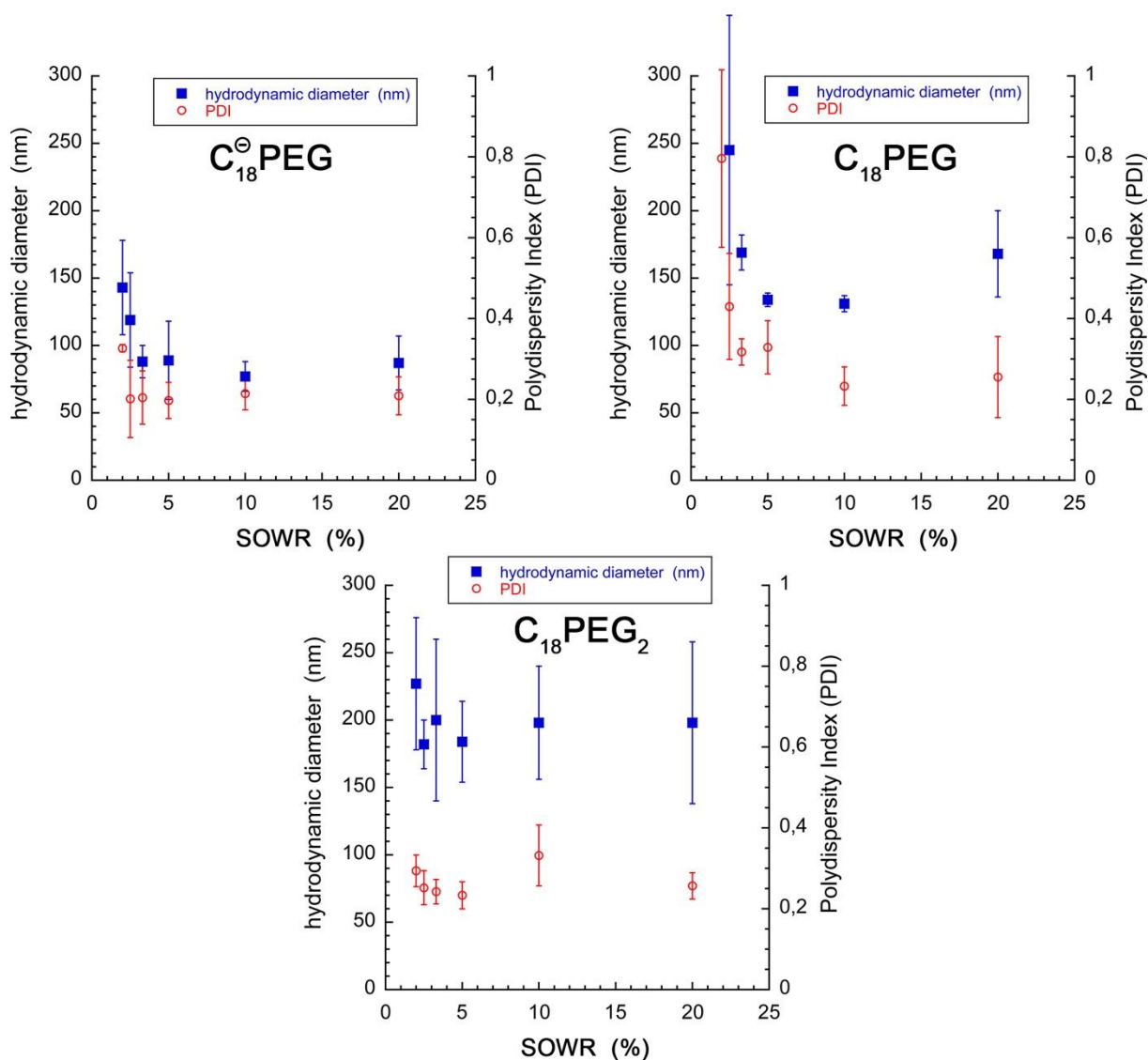
271 attributed to the increasing efficiency of surfactant at the interface, related to the interfacial
272 concentration as the bulk concentration was increased.

273 On the other hand, in Fig. 4B and Fig. 4C, for **C₁₈-PEG** and **C₁₈-PEG₂**, respectively, an opposite
274 trend arose, showing an increase of the droplet size with the SOR. These results clearly
275 contrasted with the ones generally obtained [1,14,17,26] with such processes, since, unlike
276 **C₁₈[⊖]-PEG**, in that cases the droplet size and PDI increased with increasing surfactants
277 amount. In addition, in the case of **C₁₈-PEG**, the PDI values are too high (> 0.25) for validating
278 the measurements, while they conserved a good value (< 0.25) in the case of **C₁₈-PEG₂**. In
279 both cases, emulsification process seemed to be affected by these chemical modifications.
280 The lower CMC disclosed in Fig. 3 for **C₁₈-PEG** and **C₁₈-PEG₂** might be related to this behavior,
281 indicating that a lower water solubility affected the interfacial behavior at high
282 concentrations. It is interesting to note, as well, that the process of droplet coalescence after
283 emulsification could be slowed down by their surface charge, orienting the global size
284 distribution towards smaller size range with charged molecules, as observed. This was
285 confirmed with the values of zeta potential, measured at -28 mV and -30.0 mV for **C₁₈-PEG**
286 and **C₁₈-PEG₂**, respectively, when it raised at -39 mV for the charged **C₁₈[⊖]-PEG** surfactant.

287 3.3.2 Effect of water ratio

288 The effect of water concentration was investigated by preparing a series of emulsions with
289 different SOWRs from 2% to 20%, at a fixed SOR of 50% and a fixed emulsification
290 temperature of 90°C. The results, reported in Fig. 5, overall showed a decrease and
291 stabilization of the size as the water content increased. In general, the impact of the water
292 ratio was considered as not impacting on the nano-emulsion size, and this is effectively
293 observed with SOWR ≥ 5%. On the other hand, for very high proportions of water (low
294 SOWRs) the quality of the emulsion was surprisingly decreased and size increased. This
295 feature was probably not documented since such concentration range had a limited interest.
296 However, it reveals that a minimum volume fraction of dispersed phase was required in
297 order to make efficient the spontaneous emulsification process.

298



299
 300 **Figure 5:** Size and PDI of NEs prepared using C₁₈[⊖]-PEG, C₁₈-PEG and C₁₈-PEG₂, in function of the values of SOWR,
 301 at constant SOR = 50% and at emulsification temperature T = 90°C.

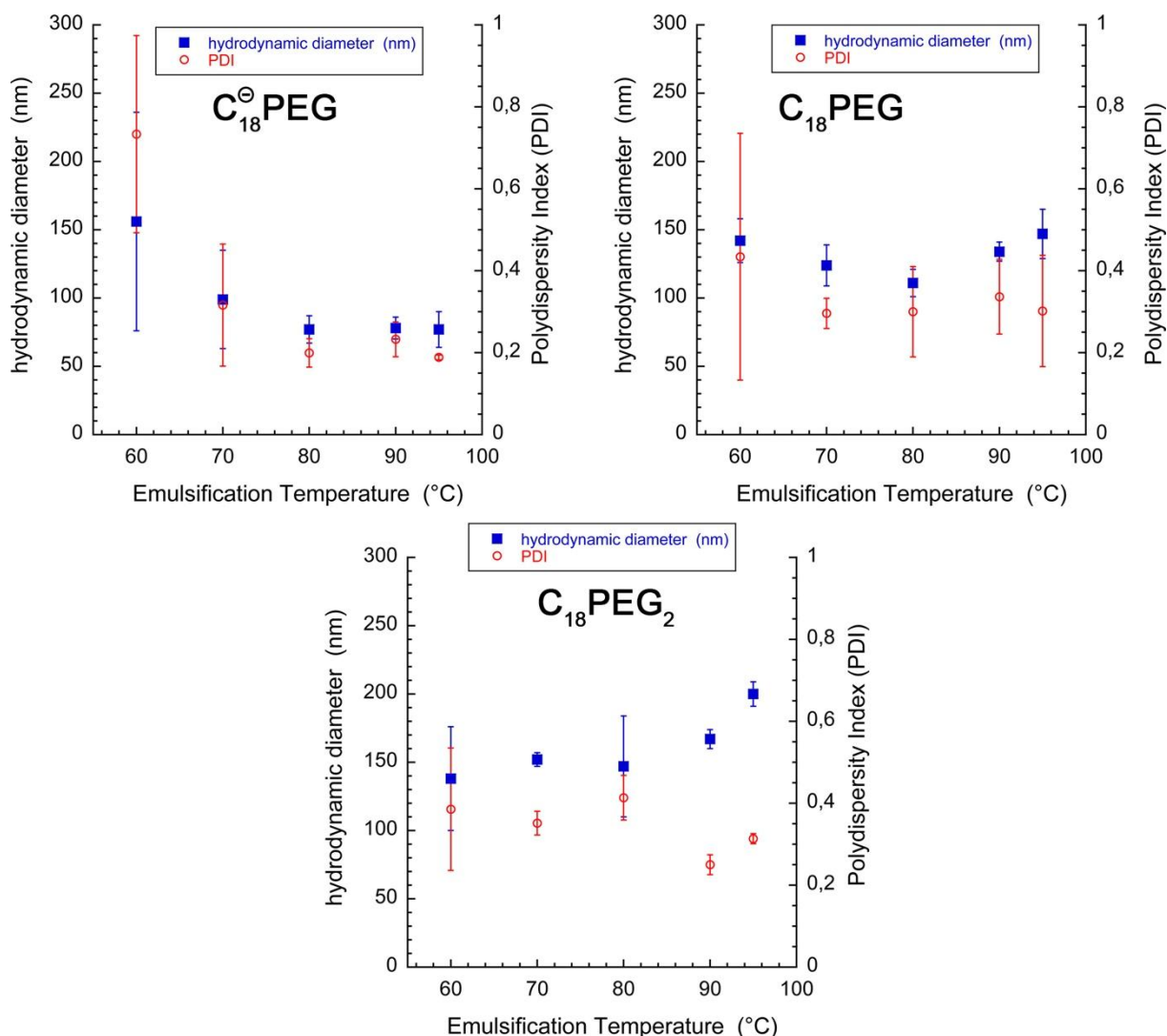
302

303 3.3.3 Effect of emulsification temperature

304 Spontaneous nano-emulsification process was based on the physico-chemical behavior of
 305 nonionic surfactants, and particularly on their temperature sensitivity [13]. Indeed, playing
 306 on temperature modified the solubility of the PEG chains and, in certain conditions, induced
 307 the spontaneous generation of droplets. In previous reported studies [1,13,27], we described
 308 the impact of the emulsification temperature on the process itself, giving the temperature
 309 threshold impacting on the process efficiency. Indeed, if the emulsification temperature was
 310 below the cloud point –or phase inversion temperature– the process dramatically lose
 311 efficiency below those temperature thresholds. In the present case of comparison, different
 312 surfactants, investigating this parameter appeared important to understand their impact on
 313 the emulsification process. To this end, emulsions were prepared from 60°C to 90 °C with a

314 fixed SOR of 50% and SOWR of 5%. Results are shown in Fig. 6. This parameter had a
315 significant impact on the nano-emulsions' properties. Considering C_{18}^{\ominus} -PEG, for $T < 80^{\circ}C$, the
316 size, PDI and reproducibility was clearly affected, when compared to $T \geq 80^{\circ}C$ where these
317 parameters were much better and reproducible. This result confirmed the thermo-sensitivity
318 and the behavior expected for such nonionic surfactants. On the other hand, this conclusion
319 could not be drawn for the other surfactants (C_{18} -PEG and C_{18} -PEG₂), for which the
320 temperature did not seem to have a real impact on the process efficiency. For these
321 surfactants, in those conditions (SOR and SOWR values), the PDI values remained quite high,
322 and we could conclude that the nano-emulsions generated did not meet quality criteria. It
323 can be explained by the surfactant's affinities for aqueous and oil phase, not optimally
324 balanced for inducing sufficient turbulences during the emulsification. Another factor that
325 could induce the un-robustness of such processes, was the oil phase viscosity transitory
326 which significantly varied with the temperature. Indeed, from $60^{\circ}C$ to $90^{\circ}C$, VEA viscosity
327 decreased almost four times [28], which could impact on the properties of droplets
328 fractionation.

329



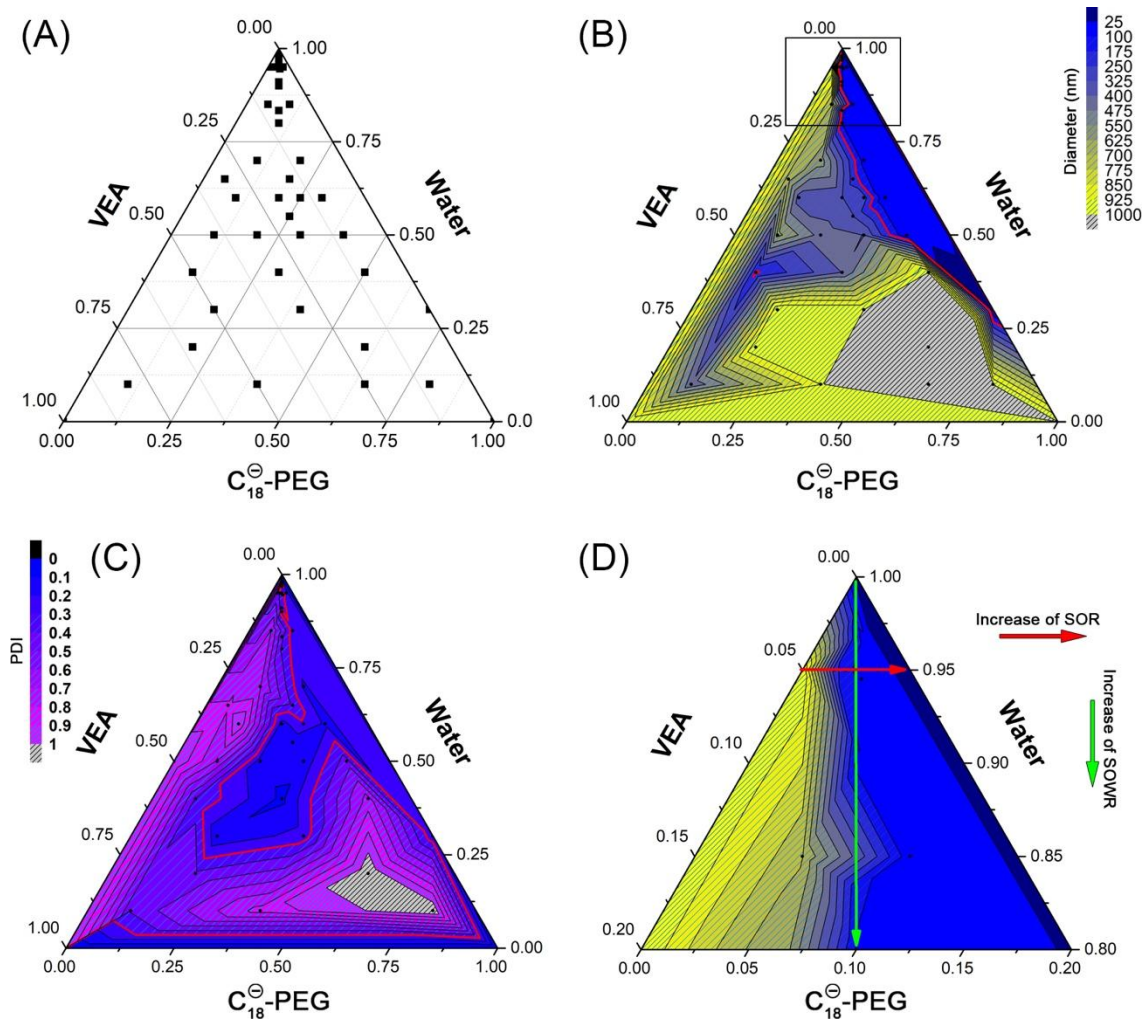
330
 331 **Figure 6:** Size and PDI of NEs prepared using C₁₈[⊖]-PEG, C₁₈-PEG and C₁₈-PEG₂, in function of the values of
 332 emulsification temperature, at constant SOR = 50% and SOWR = 5%.

333 3.4 Optimization of nano-emulsification process

334 To gain further insights into the spontaneous emulsification process obtained with these new
 335 surfactants, a screening of formulations (38 different formulations, see Fig. 7 (A)) was
 336 undertaken and compared each other. This part focused on the C₁₈[⊖]-PEG, that showed the
 337 best nano-emulsions, and allowed comparing finely the impact of the composition on the
 338 emulsification process. The corresponding results, as size distribution and PDI, are shown in
 339 Fig. 7 (B) and (C), respectively. In Fig. 7 (B), the red line delimited the region where emulsions
 340 are sizing below 250 nm, thus, so-called *nano-emulsions*. The small zones indicated with
 341 deepen blue showed sizes below 25 nm, possibly small nano-emulsions, but could also be
 342 swollen micelles (micelles swollen by oil [27]). The main results given by Fig. 7 (B) are (i)
 343 nano-emulsions feasibility domain overall corresponded to low oil ratio, below 25%.
 344 Increasing of oil quantity resulted in the lack of surfactant coverage of the oil-water interface;
 345 (ii) On the other hand, an excess of surfactant (with reduction of water), formed a

346 concentrated surfactant phase containing high amount of micelles, and for the most
 347 concentrated regions, turned into *gel phase* probably forming liquid crystalline phases
 348 [29,30]. In Fig. 7 (C), the red line emphasized the region of PDI values lower than 0.3, for
 349 which we considered the population monodisperse and stable. In Fig. 7 (D), the focus was
 350 done on the water corner of Fig. 7 (B), showing the nano-emulsification in the more diluted
 351 conditions, up to SOWR equal to 20 %. Red and green arrows indicated the increase of SOR
 352 and SOWR, respectively. Such region corresponds to the emulsification studied above and
 353 confirmed that nano-emulsification process is mainly driven by surfactant amount, with a
 354 weak influence of the other formulation parameters.

355



356

357 **Figure 7** Investigation of the composition on the emulsification of C_{18}^{\ominus} -PEG, with the ternary system composed
 358 of C_{18}^{\ominus} -PEG (surfactant), oil (VEA vitamin E acetate) and water. (A) Screening of the formulations studied, (B)
 359 Values of the mean size of the droplet population (hydrodynamic diameter). (C) PDI values corresponding to the
 360 results reported in part (B). (D) Focus on the water corner of part (B), indicated with a square.

361

362 In this study, we mainly focused the investigation on the potentials offered by OSA
 363 derivatives. OSA readily led to amphiphilic molecules which could easily be modified as

364 derivatives with modulated properties that showed the potential to act as an emulsifier. It is
365 noteworthy that such approaches have been approved by the FDA for use in food industry,
366 for example in the case of OSA starches used as emulsifiers and encapsulating agents which
367 can form emulsions with an average size around 500 μm [31]. In addition, one advantage of
368 these derivative owed to their independency of ionic strength [32].

369

370

371 **4 Conclusion**

372 In this study, we synthesized new amphiphilic molecules and studied their ability for
373 generating emulsions and nano-emulsions by spontaneous emulsification method. Based on
374 a common basis of OSA as monomeric entity, the variations in the surfactant molecules were
375 done on the hydrophilic moiety, through the addition of one or two Jeffamine chains in
376 different configurations, so-called **C₁₈[⊖]-PEG**, **C₁₈-PEG** and **C₁₈-PEG₂**. This study not only shows
377 the simplicity of the chemical modification of OSA, but also the significant impact on the
378 spontaneous process and properties of the droplet population. The comparison of these
379 three surfactants, gave that **C₁₈[⊖]-PEG** performed the smallest size distribution and lowest
380 PDI values. From the structure-activity point of view, HLB values are globally calculated in
381 comparable range, whereas regarding the CMC, **C₁₈[⊖]-PEG** appears more hydrophilic
382 compared to **C₁₈-PEG** and **C₁₈-PEG₂**, very close each other. As the spontaneous emulsification
383 process is related to the balance between surfactant affinity for oil and aqueous phases, this
384 point could explain the slight difference between process efficiency revealed. From an
385 optimization experiment, we disclosed that the best conditions are included in the lower
386 surfactant concentrations, for water and oil contents higher and lower than 50%,
387 respectively. Among all the factors impacting on the spontaneous emulsification, a larger
388 SOR and a higher emulsification temperature could benefit the fabrication, while SOWR had
389 limited influence.

390

391 **5 Acknowledgements**

392 The authors thank the China Scholarship Council for funding Ph.D. fellowship for X.W., (CSC
393 No. 201706240033).

394 **6 References**

395 [1] N. Anton, T.F. Vandamme, The universality of low-energy nano-emulsification, *Int. J.*
396 *Pharm.* 377 (2009) 142–147.

- 397 <https://doi.org/https://doi.org/10.1016/j.ijpharm.2009.05.014>.
- 398 [2] X. Li, N. Anton, G. Zuber, T. Vandamme, Contrast agents for preclinical targeted X-ray
399 imaging, *Adv. Drug Deliv. Rev.* 76 (2014) 116–133.
400 <https://doi.org/10.1016/j.addr.2014.07.013>.
- 401 [3] Y. Singh, J.G. Meher, K. Raval, F.A. Khan, M. Chaurasia, N.K. Jain, M.K. Chourasia,
402 Nanoemulsion: Concepts, development and applications in drug delivery, *J. Control.*
403 *Release.* 252 (2017) 28–49.
404 <https://doi.org/https://doi.org/10.1016/j.jconrel.2017.03.008>.
- 405 [4] O. Sonnevile-Aubrun, M.N. Yukuyama, A. Pizzino, Chapter 14 - Application of
406 Nanoemulsions in Cosmetics, in: S.M. Jafari, D.J. McClements (Eds.), *Nanoemulsions*,
407 Academic Press, 2018: pp. 435–475. [https://doi.org/https://doi.org/10.1016/B978-0-](https://doi.org/https://doi.org/10.1016/B978-0-12-811838-2.00014-X)
408 [12-811838-2.00014-X](https://doi.org/https://doi.org/10.1016/B978-0-12-811838-2.00014-X).
- 409 [5] L. Wang, X. Li, G. Zhang, J. Dong, J. Eastoe, Oil-in-water nanoemulsions for pesticide
410 formulations, *J. Colloid Interface Sci.* 314 (2007) 230–235.
411 <https://doi.org/https://doi.org/10.1016/j.jcis.2007.04.079>.
- 412 [6] D.J. McClements, J. Rao, Food-Grade Nanoemulsions: Formulation, Fabrication,
413 Properties, Performance, Biological Fate, and Potential Toxicity, *Crit. Rev. Food Sci.*
414 *Nutr.* 51 (2011) 285–330. <https://doi.org/10.1080/10408398.2011.559558>.
- 415 [7] R. Bouchaala, L. Mercier, B. Andreiuk, Y. Mély, T. Vandamme, N. Anton, J.G. Goetz, A.S.
416 Klymchenko, Integrity of lipid nanocarriers in bloodstream and tumor quantified by
417 near-infrared ratiometric FRET imaging in living mice, *J. Control. Release.* 236 (2016).
418 <https://doi.org/10.1016/j.jconrel.2016.06.027>.
- 419 [8] N. Anton, T.F. Vandamme, Nano-Emulsions, in: M. Aliofkhazraei (Ed.), *Handb.*
420 *Nanoparticles*, Springer International Publishing, Cham, 2016: pp. 93–116.
421 https://doi.org/10.1007/978-3-319-15338-4_2.
- 422 [9] Z. Li, D. Xu, Y. Yuan, H. Wu, J. Hou, W. Kang, B. Bai, Advances of spontaneous
423 emulsification and its important applications in enhanced oil recovery process, *Adv.*
424 *Colloid Interface Sci.* 277 (2020) 102119.
425 <https://doi.org/https://doi.org/10.1016/j.cis.2020.102119>.
- 426 [10] C. Solans, D. Morales, M. Homs, Spontaneous emulsification, *Curr. Opin. Colloid*
427 *Interface Sci.* 22 (2016) 88–93.
428 <https://doi.org/https://doi.org/10.1016/j.cocis.2016.03.002>.
- 429 [11] J.C. López-Montilla, P.E. Herrera-Morales, S. Pandey, D.O. Shah, Spontaneous
430 Emulsification: Mechanisms, Physicochemical Aspects, Modeling, and Applications, *J.*
431 *Dispers. Sci. Technol.* 23 (2002) 219–268.
432 <https://doi.org/10.1080/01932690208984202>.
- 433 [12] A. Gupta, Z. Badruddoza, P.S. Doyle, A General Route for Nanoemulsion Synthesis
434 using Low Energy Methods at Constant Temperature, *Langmuir.* 33 (2017) 7118–7123.
435 <https://doi.org/10.1021/acs.langmuir.7b01104>.
- 436 [13] N. Anton, S. Akram, T.F. Vandamme, Chapter 4 - Transitional Nanoemulsification
437 Methods, in: S.M. Jafari, D.J. McClements (Eds.), *Nanoemulsions*, Academic Press,

- 438 2018: pp. 77–100. [https://doi.org/https://doi.org/10.1016/B978-0-12-811838-](https://doi.org/https://doi.org/10.1016/B978-0-12-811838-2.00004-7)
439 2.00004-7.
- 440 [14] M.F. Attia, N. Anton, M. Chiper, R. Akasov, H. Anton, N. Messaddeq, S. Fournel, A.S.
441 Klymchenko, Y. Mély, T.F. Vandamme, Biodistribution of X-ray iodinated contrast agent
442 in nano-emulsions is controlled by the chemical nature of the oily core, *ACS Nano*. 8
443 (2014) 10537–10550. <https://doi.org/10.1021/nn503973z>.
- 444 [15] X. Li, N. Anton, T.M. Ta, M. Zhao, N. Messaddeq, T.F. Vandamme, Microencapsulation
445 of nanoemulsions: novel Trojan particles for bioactive lipid molecule delivery., *Int. J.*
446 *Nanomedicine*. 6 (2011).
- 447 [16] X. Wang, N. Anton, P. Ashokkumar, H. Anton, T.K. Fam, T. Vandamme, A.S. Klymchenko,
448 M. Collot, Optimizing the Fluorescence Properties of Nanoemulsions for Single Particle
449 Tracking in Live Cells., *ACS Appl. Mater. Interfaces*. 11 (2019) 13079–13090.
450 <https://doi.org/10.1021/acsami.8b22297>.
- 451 [17] X. Li, N. Anton, G. Zuber, M. Zhao, N. Messaddeq, F. Hallouard, H. Fessi, T.F.
452 Vandamme, Iodinated α -tocopherol nano-emulsions as non-toxic contrast agents for
453 preclinical X-ray imaging, *Biomaterials*. 34 (2013) 481–491.
454 <https://doi.org/10.1016/j.biomaterials.2012.09.026>.
- 455 [18] N. Anton, A. Parlog, G. Bou About, M.F. Attia, M. Wattenhofer-Donzé, H. Jacobs, I.
456 Goncalves, E. Robinet, T. Sorg, T.F. Vandamme, Non-invasive quantitative imaging of
457 hepatocellular carcinoma growth in mice by micro-CT using liver-targeted iodinated
458 nano-emulsions, *Sci. Rep.* 7 (2017). <https://doi.org/10.1038/s41598-017-14270-7>.
- 459 [19] Y. Chevalier, New surfactants: new chemical functions and molecular architectures,
460 *Curr. Opin. Colloid Interface Sci.* 7 (2002) 3–11.
461 [https://doi.org/https://doi.org/10.1016/S1359-0294\(02\)00006-7](https://doi.org/https://doi.org/10.1016/S1359-0294(02)00006-7).
- 462 [20] E. Bouyer, G. Mekhloufi, V. Rosilio, J.-L. Grossiord, F. Agnely, Proteins, polysaccharides,
463 and their complexes used as stabilizers for emulsions: Alternatives to synthetic
464 surfactants in the pharmaceutical field?, *Int. J. Pharm.* 436 (2012) 359–378.
465 <https://doi.org/https://doi.org/10.1016/j.ijpharm.2012.06.052>.
- 466 [21] Y. Xia, H. He, X. Liu, D. Hu, L. Yin, Y. Lu, W. Xu, Redox-responsive{,} core-crosslinked
467 degradable micelles for controlled drug release, *Polym. Chem.* 7 (2016) 6330–6339.
468 <https://doi.org/10.1039/C6PY01423B>.
- 469 [22] J. Davies, A quantitative kinetic theory of emulsion type. I. Physical chemistry of the
470 emulsifying agent. in *Gas/Liquid and Liquid/Liquid Interface*, in: *Proc. Int. Congr. Surf.*
471 *Act.*, 1957: pp. 426–438.
- 472 [23] A.U. Rehman, M. Collot, A.S. Klymchenko, S. Akram, B. Mustafa, T. Vandamme, N.
473 Anton, Spontaneous nano-emulsification with tailor-made amphiphilic polymers and
474 related monomers, *Eur. J. Pharm. Res.* 1 (2019) 27–36.
- 475 [24] P. Mukerjee, A. Ray, THE EFFECT OF UREA ON MICELLE FORMATION AND
476 HYDROPHOBIC BONDING, *J. Phys. Chem.* 67 (1963) 190–192.
477 <https://doi.org/10.1021/j100795a046>.
- 478 [25] A.H. Saberi, Y. Fang, D.J. McClements, Fabrication of vitamin E-enriched

- 479 nanoemulsions: Factors affecting particle size using spontaneous emulsification, J.
480 Colloid Interface Sci. 391 (2013) 95–102.
481 <https://doi.org/https://doi.org/10.1016/j.jcis.2012.08.069>.
- 482 [26] M.F. Attia, N. Anton, R. Akasov, M. Chiper, E. Markvicheva, T.F. Vandamme,
483 Biodistribution and toxicity of X-ray iodinated contrast agent in nano-emulsions in
484 function of their size, Pharm. Res. 33 (2016) 603–614.
485 <https://doi.org/10.1007/s11095-015-1813-0>.
- 486 [27] N. Anton, T.F. Vandamme, Nano-emulsions and micro-emulsions: Clarifications of the
487 critical differences, Pharm. Res. 28 (2011) 978–985. [https://doi.org/10.1007/s11095-](https://doi.org/10.1007/s11095-010-0309-1)
488 [010-0309-1](https://doi.org/10.1007/s11095-010-0309-1).
- 489 [28] E. Szwajczak, J. Świergiel, R. Stagraczyński, J. Jadzyn, Viscous and dielectric properties
490 of α -tocopherol and α -tocopherol acetate, Phys. Chem. Liq. 47 (2009) 460–466.
491 <https://doi.org/10.1080/00319100902737455>.
- 492 [29] P. Saulnier, N. Anton, B. Heurtault, J.-P. Benoit, Liquid crystals and emulsions in the
493 formulation of drug carriers, Comptes Rendus Chim. 11 (2008).
494 <https://doi.org/10.1016/j.crci.2007.10.005>.
- 495 [30] N. Anton, J.-P. Benoit, P. Saulnier, Particular conductive behaviors of emulsion phase
496 inverting, J. Drug Deliv. Sci. Technol. 18 (2008). [https://doi.org/10.1016/S1773-](https://doi.org/10.1016/S1773-2247(08)50015-3)
497 [2247\(08\)50015-3](https://doi.org/10.1016/S1773-2247(08)50015-3).
- 498 [31] Y. Hong, Z. Li, Z. Gu, Y. Wang, Y. Pang, Structure and emulsification properties of
499 octenyl succinic anhydride starch using acid-hydrolyzed method, Starch - Stärke. 69
500 (2017) 1600039. <https://doi.org/https://doi.org/10.1002/star.201600039>.
- 501 [32] L. Altuna, M.L. Herrera, M.L. Foresti, Synthesis and characterization of octenyl succinic
502 anhydride modified starches for food applications. A review of recent literature, Food
503 Hydrocoll. 80 (2018) 97–110.
504 <https://doi.org/https://doi.org/10.1016/j.foodhyd.2018.01.032>.
- 505